Songklanakarin J. Sci. Technol.
35 (6), 693-703, Nov. - Dec. 2013

SJST SONGKLANAKARIN JOURNAL OF SCIENCE AND TECHNOLOGY
http://www.sjst.psu.ac.th

Original Article

Microstructure and mechanical properties of microwave-assisted heating of pozzolan-Portland cement paste at a very early stage

Natt Makul[1]* and Dinesh Kumar Agrawal[2]

[1] *Department of Building Technology, Faculty of Industrial Technology, Phranakhon Rajabhat University, Bang Khen, Bangkok, 10220 Thailand.*

[2] *Department of Engineering Science and Mechanics, Materials Research Laboratory, The Pennsylvania State University, Pennsylvania, 16802 USA.*

Received 27 February 2012; Accepted 28 August 2013

Abstract

Portland-pozzolan cement pastes at a very early stage subjecting to microwave heating were investigated. Microwave with a 2.45 GHz and multimode cavity was used for the experiments. The pastes containing pozzolan materials (pulverized fuel ash, metakaolin and silica fume) were proportioned with a 0.38 water/solid mass ratio and a 20% by weight replacement of total solid content. It was observed that the temperature increased continuously during microwave heating. Some ettringite rods and amorphous C-S-H fibers appear at 4 hrs. The metakaolin-cement paste exhibited little difference between the water-cured and microwave-cured pastes. For the silica fume-cement paste the SF particles under microwave curing had dispersed more than with the 4 hr–cement paste. The produced phases included calcium silicate hydrate, calcium hydroxide and xenotile. The pastes can be developed in compressive strength quite rapidly and also consumed more $Ca(OH)_2$ in the pozzolan reaction to produce more C-S-H.

Keywords: microwave, microstructure, Portland cement, paste, pozzolan

1. Introduction

Microwave energy has been widely used as a mature technique with wide-ranging industrial applications especially the operating frequencies of 0.915 and 2.45 GHz as assigned by the International Telecommunication Union (ITU) are most often used for industrial, scientific, and medical (ISM) purposes in the range from 433.92 MHz to 40 GHz. With selective and volumetric heating, microwave sintering can enhance efficiency and reduce processing time of sintering process considerably and thereby save energy. Some achievements with such advantages have been demonstrated in ceramics (Metaxas, 1991; Jae-Hwan *et al.*, 2001; Padma *et al.*, 2009), tempering frozen meat (Göksoy *et al.*, 2000; Taher and Farid, 2001), curing adhesives for lumber (Beall, 2007), food processing (Peyre *et al.*, 1997; Orsat, 2007; Chen, 2008), bonding composite sheets (Sgriccia and Hawley, 1991; Zhu *et al.*, 2007), removing contaminated surfaces (Li *et al.*, 1994; Basak and Durairaj, 2001), treating hyperthermia (Arunachalam, 2008), and others.

The use of microwave energy to improve the properties of Portland cement-based materials is a relatively new area of research (Hutchison *et al.*, 1991; Leung and Pheeraphan, 1995; Makul *et al.*, 2009), particularly for accelerated curing applications. Conventional heating methods possess disadvantages such as extended time for strength development (American Concrete Institute, 2005) and reduced final strength due to excessive heating. While appropriate application of heat aids in temperature control during hydration, use of these techniques requires strict attention to specifications

* Corresponding author.
Email address: shinomomo7@hotmail.com

and established application procedures to ensure proper performance and long-term durability (American Concrete Institute, 2005).

Concrete is conventionally composed of dielectric materials capable of effectively absorbing microwave energy, including Portland cement, aggregates, water, and admixtures. In particular, water has a high relative dielectric constant (ε_r') and loss tangent (tan δ), and when the electric field $(\vec{E})$ component of electromagnetic radiation interacts with concrete the energy is transferred and converted into heat primarily via interactions with water molecules. The heat input accelerates hydration reactions within the concrete, leading to removal of free water molecules within the capillary pores of the concrete before setting. The water removal causes plastic shrinkage, collapse of the capillary pores, and densification of the microstructure. Equation 1 describes the relationship between field intensity and available energy:

$$Q = \sigma\left|\vec{E}\right|^2 = 2\pi f \varepsilon_0 \varepsilon_r^{'} \left(\tan\delta\right)\left|E\right|^2 \quad (1)$$

Here Q is the microwave energy, s is the effective conductivity, f is the frequency (Hz), e_0 is the permittivity of free space (8.8514×10^{-12} F/m), $\varepsilon_r^{'}$ is the relative dielectric constant, tan δ is the loss tangent coefficient, and $\vec{E}$ is the electric field intensity (V/M).

Dielectric behavior may be analyzed using two independent electromagnetic properties: the complex electric permittivity ε^* (Equation 2) and the complex magnetic permeability μ^*. Most common concrete materials are non-magnetic and have permeabilities very close to the permeability of free space ($\mu_o = 4\pi x 10^{-7}$ Henry/meter) (Metaxas, 1991; Makul *et al.*, 2009), and their dielectric behavior may be described using only the complex electric permittivity. This parameter is composed of real and imaginary parts defined by:

$$\varepsilon_r^* = \varepsilon_r' - \vec{j}\varepsilon_r'' \quad (2)$$

in which ε_r' and ε_r'' are the real and imaginary parts of the complex permittivity and $\vec{j} = \sqrt{-1}$. The real part of the relative complex permittivity is referred to as the dielectric constant ε_r' and is a measure of how much of the energy transferred from an external electric field and is stored in a material. The imaginary component ε_r'' indicates the dielectric loss of a material in the presence of an external electric field and is referred to as the relative loss factor which is responsible for the heat generated. The ratio between the energy lost (relative loss factor) to the energy stored (relative dielectric constant) in a material is also an important parameter and is known as the loss tangent tan δ, Equation 3:

$$\tan\delta = \varepsilon_r'' / \varepsilon_r' \quad (3)$$

Pozzolan materials have been used in construction applications for many years as partial substitutes for Portland cement. Use of these materials may enhance various properties of cement and concrete and reduces CO_2 emission during cement production. Popular pozzolan materials include pulverized fuel ash (FA), metakaolin (MK), and silica fume (SF). For example, FA improves concrete workability, lowers water requirements, reduces heat of hydration, reduces permeability and adsorption of the finished concrete, and is economical (Kim and Lee, 2011), metakaolin (Badogiannis *et al.*, 2005) can increase strength and reduce permeability, and silica fume improves the properties of fresh and hardened concrete such as strength and density (Bhanja and Sengupta, 2003). However, concrete mixtures containing these materials require additional processing for performance enhancement, for example heating during the early stages of the hydration reaction. However, thermal curing methods may lead to early-stage and long-term drawbacks such as micro-cracking or delayed ettringite formation (Verbeck and Helmuth, 1969). Microwave heating may circumvent these problems since the heating in microwave processes occurs from inside the sample.

Previous studies have clearly demonstrated that microwave heating leads to unique microstructural characteristics including an increase in the early-age strength of cement-based materials (Moukwa *et al.*, 1991; Dongxu and Xuequan, 1994). However, the effect of microwave-accelerated curing of Portland cement incorporating pozzolan materials has not been fully investigated. In order to address some of this gap, we examined the effect of 2.45 GHz multimode microwave heating on cement pastes containing fuel ash, metakaolin, or silica fume.

2. Experimental Program

2.1 Materials

Type 1 hydraulic Portland cement, pulverized fuel ash, metakaolin, and silica fume were used throughout this study. Their chemical compositions and physical properties are listed in Table 1. The ASTM C 618 (American Society for Testing and Materials, 2009a) classifies the FA as low calcium content (Type F) and metakaolin. Silica fume was also used as a high-pozzolan material in accordance with the ASTM C 1240 (American Society for Testing and Materials, 2009b). Deionized water with a pH 7.5 and a high range water reducing admixture as well known as superplasticizer, conformed to the ASTM C 494 (American Society for Testing and Materials, 2009a) were also used. The sizes of the Portland cement and FA particles as shown in Figure 1 were obtained using a micrograph sedigraph instrument. The method is based on X-Ray power attenuation, which is suspended in a sample cell and allowed to settle. Studies performed using the Malvern instrument Mastersizer 2000 particle size analyzer have achieved accuracy of ±1% as designated by the median particle diameter (d_{50}) using the Malvern quality audit standard.

2.2 Sample preparation

The pastes were proportioned at a water-to-solid mass ratio of 0.38 as shown in Table 2. Herein, the superplasticizer

Table 1. Chemical composition and physical properties of cement constituents.

	Type 1 Portland Cement(OPC)	Pulverized fuel ash (FA)	Metakaolin (MK)	Silica fume (SF)
Chemical composition (% by mass)				
Silicon dioxide (SiO_2)	20.30	47.80	55.14	96.00
Aluminum oxide (Al_2O_3)	5.67	22.70	43.95	0.10
Ferric oxide (Fe_2O_3)	6.23	21.90	0.75	0.10
Magnesium oxide (MgO)	3.14	0.92	0.40	0.13
Calcium oxide (CaO)	60.43	2.18	0.08	0.12
Sodium oxide (Na_2O)	0.36	0.32	0.05	0.10
Potassium oxide (K_2O)	0.90	2.15	2.10	0.45
Sodium oxide (SO_3)	2.80	0.37	0.05	0.02
Physical properties				
Loss on Ignition	1.80	1.44	12.50	2.57
Particle size (d_{50}, µm)	49.27	223.50	285.12	0.68
Specific gravity	3.12	2.45	2.25	2.90
Specific surface area (Brunauer, Emmett and Telle, BET) (m^2/kg)	0.85	0.70	0.60	18.02

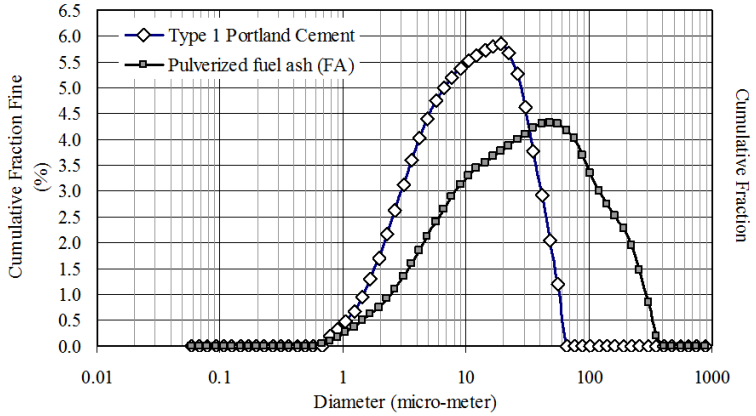

(a) Type 1 Portland cement and pulverized fuel ash.

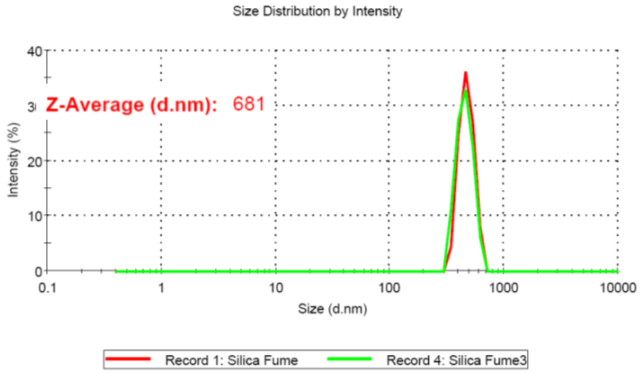

(b) Silica fume (SF)

Figure 1. Particle size distributions of Type 1 Portland cement, FA, and SF.

Table 2. Mixture proportions for cement samples.

Type of Paste	Water/solid mass ratio	OPC	FA	MK	SF	Water	Superplasticizer
		(g)	(g)	(g)	(g)	(g)	% of solid content
Type 1 cement paste	0.38	1000	-	-	-	380	1.0
FA20S	0.38	800	200	-	-	380	1.0
MK20S	0.38	800	-	200	-	380	1.0
SF20S	0.38	800	-	-	200	380	1.0

was used as a recommended dosage rate of 1% of total solid content. After mixing and molding, they were cured at room temperature by wrapping with polyethylene plastic until the delay time (time after mixing until introducing microwave energy with a multi-mode cavity) of 30 min. A Hobart mixer was used to mix the solids and liquids according to ASTM C 305 (American Society for Testing and Materials, 2009b). A total of 84 cylindrical samples 41.0 mm in diameter and 34.0 mm tall (Figure 2) were prepared.

2.3 Heating methods

The microwave heating system used in this study is shown in Figure 3 that includes an industrial microwave generator model S56F. This model can generate microwave energy at 2.45±0.05 GHz and a maximum power of 6.0 kW into a multimode applicator. This microwave apparatus does not provide real-time monitoring of temperature changes during microwave curing; therefore, the temperature of the sample was measured at the start and end of the curing process. In order to measure the temperature of the sample subjected to microwave energy, the positions of measurement were determined. Microwave energy at a power of 390 W for 45 min application time and 30 min delay time after mixing the paste specimens was employed that is an optimal condition from preliminary study. The temperature of the top surface and the bottom surface was measured five times for each; likewise, the sample was immediately fractured and inside temperature was also measured five times. For water curing method, the paste samples were cured until testing time by saturated-lime deionized water at 25°C to compare the characteristics of microwave-cured pastes.

2.4 Test procedures

Dielectric measurements were obtained using the transmission/reflection-line technique, which involves placing the sample in a section of waveguide or coaxial line and measuring the complex scattering parameters at the two ports. A calibration procedure must be carried out before making the measurements in which the reflected (S_{11}) and transmitted signals (S_{21}) are measured. The complex permittivity and permeability of the material may be determined from the scattering parameters. A vector network analyzer (VNA, HP 8510) (Hewlett Packard Corporation, 1992) was used to measure the dielectric properties of the paste samples. As with all network analyzers, the HP 8510 is capable of both reflection and transmission measurements, Figure 4(a) and (b). An incident signal generated using an RF source was compared with the signal transmitted through the analyzer or reflected from the input, Figure 4(c). The conversion of S measurements to complex

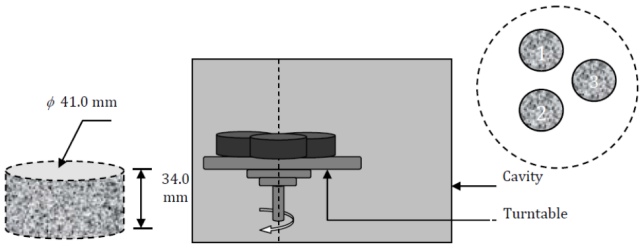

Figure 2. Specimen geometry and arrangement within microwave cavity.

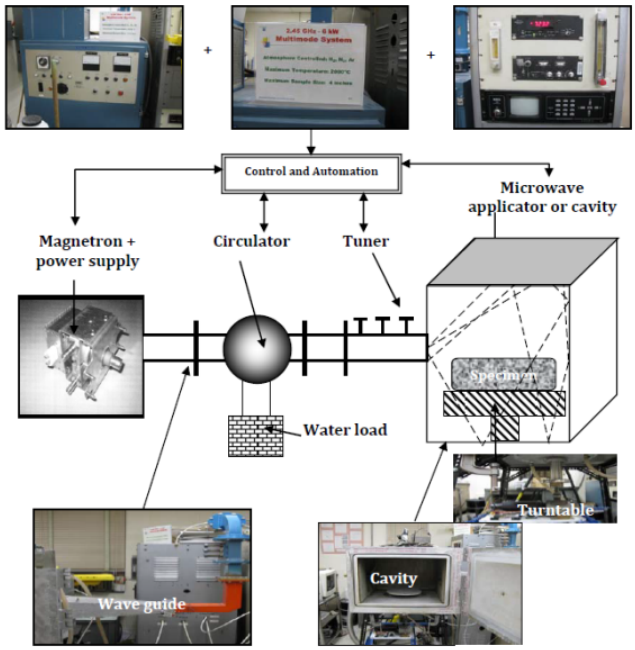

Figure 3. Configuration of microwave heating apparatus.

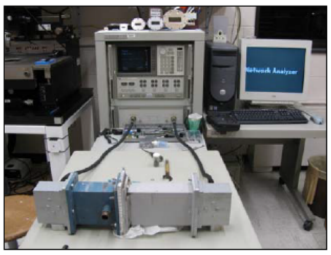

(a) Vector network analyzer (VNA, HP 8510)

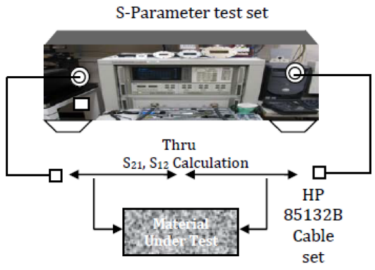

(b) Schematic of VNA

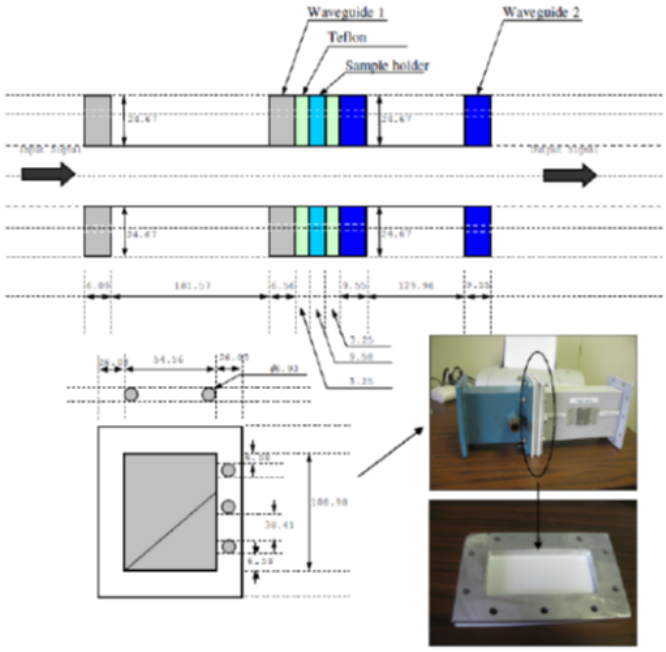

(c) Waveguide

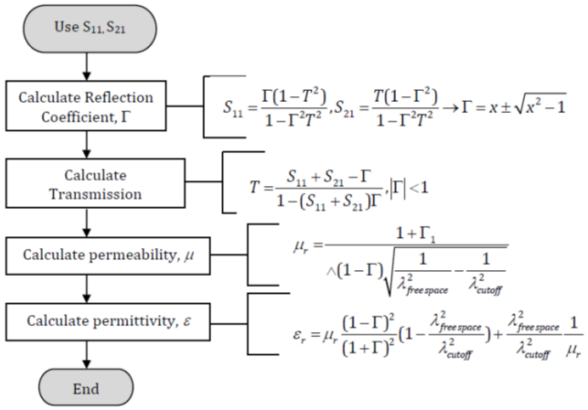

(d) Nicholson–Ross–Weir method for calculating dielectric permittivity.

Figure 4. Network analyzer and waveguide details.

dielectric parameters was accomplished using the Nicholson-Ross-Weir (NRW) technique (Venkatesh and Raghevan, 2005) (Figure 4(d)).

A Scanning Electron Microscope (SEM) associated with energy dispersive X-ray spectroscopy, specifically an International Scientific Instruments ISI-130 electron microscope, was used to determine the microstructure and morphology of the samples. The crystalline phase identification of the various samples was performed on a Scintag X-ray Diffractometer. This differactometer is equipped with a copper

target X-ray source, monochromator, and Tl-drifted NaI scintillation detector. Dried-powder samples were packed into a cavity of a zero-background quartz slide and placed on a goniometry. Most of the subsequent scans were taken from 25 to 45° 2θ at a rate of 2° 2θ per minute. The compressive strengths of the cement pastes were determined using a compressive strength apparatus in accordance with the ASTM C 39 (American Society for Testing and Materials, 2009a) at the ages of 8 and 24 hrs, and 3 and 28 days.

3. Results and Discussion

3.1 Dielectric properties

Figure 5 describes the evolution of the dielectric permittivity of the paste samples through the first 24 hrs of hydration time. The dielectric permittivity during the initial stages was relatively high in comparison with later stages. The dielectric properties of the cement-pozzolan mixtures were higher than those of the control paste. In particular, the FA20S paste contained more free water due to the slower pozzolan reaction of fly ash in comparison to silica fume and metakaolin leads to slower consumption of water. As a result, there is more water remaining in the mix. This resulted in increased dissolution of polarized ions (Ca^{2+} and OH^-), increasing the dielectric constant of the paste (Wittmann and Schlude, 1975). Both silica fume and fly ash underwent pozzolan reactions. The MK20S paste exhibited behavior similar to the SF20S and FA20S pastes. The difference in loss factor between the control paste and SF20S paste was relatively low, and was considerably larger for the FA20S and MK20S pastes, indicating residual water content in both materials during the dormant and acceleratory periods. The FA20S paste samples retained high loss factor for a longer period of time due to the greater amount of free water in this material. In both samples, we found that a high dielectric permittivity means the paste is in a liquid state. At later stages, when the pastes achieve low dielectric permittivity, they are in the hardened state.

As shown in Figure 5, the dielectric permittivities of the cement-pozzolan pastes change more drastically than that of the control paste. This evolution indicates that the dielectric permittivity affects the overall microwave heat generation in the bulk paste, as well as the penetration depth of the radiation (Makul *et al.*, 2009). Consider that the microwave energy is only applied for 45 minutes, starting half an hour after mixing. Measuring the dielectric permittivity of the paste half an hour after mixing can therefore provide valuable information on the amount of heat generated, and hence the quality of the hydration and pozzolan reaction products. On the other hand, measuring the dielectric permittivity of the FA20S, MK20S and SF20S pastes at regular intervals up to 24 hrs after mixing provides information helping to establish the most suitable method of microwave-accelerated curing.

3.2 Temperature and power evolution

The temperature profiles of the Type 1 cement paste and cement-pozzolan pastes at a microwave power of 390 W with a specific application time of 45 min half an hour after mixing are shown in Figure 6. The temperature profiles were obtained by averaging the five monitored data at the top surface, at the bottom surface and in the inside of the specimen. According to the data the temperature increases monotonically during the microwave-curing process and reached a maximum temperature of 89°C at the bottom surface of the microwave-cured FA20S paste, 72.9°C at the bottom surface of the microwave-cured MK20S paste, and 62.4°C at the bottom surface of the microwave-cured SF20S paste. Significantly, for pastes containing pozzolan temperature rise relates to the free water that was not absorbed by the pozzolan, and the amount of heat that microwave energy generates is also decreased as well. It is well-known that the FA particles are more rounded in shape than the MK and SF particles, and as a result the FA20S paste shows the highest temperature increase among the three.

Furthermore, at early-age microwave curing, the rate at which the temperature increases is higher than the sequential temperature profile of the FA20S paste. This is due to the fact that microwave energy accelerates rapidly the hydration (Moukwa *et al.*, 1991) and pozzolan reactions and thus affects the production of Portlandite ($Ca(OH)_2$). This is subsequent to an increase in the concentration of Portlandite, which, in turn, also speeds up the pozzolan reaction. It should be noted

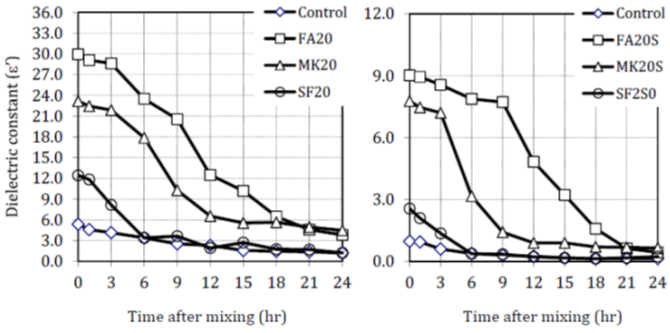

Figure 5. Dielectric permittivity of paste samples.

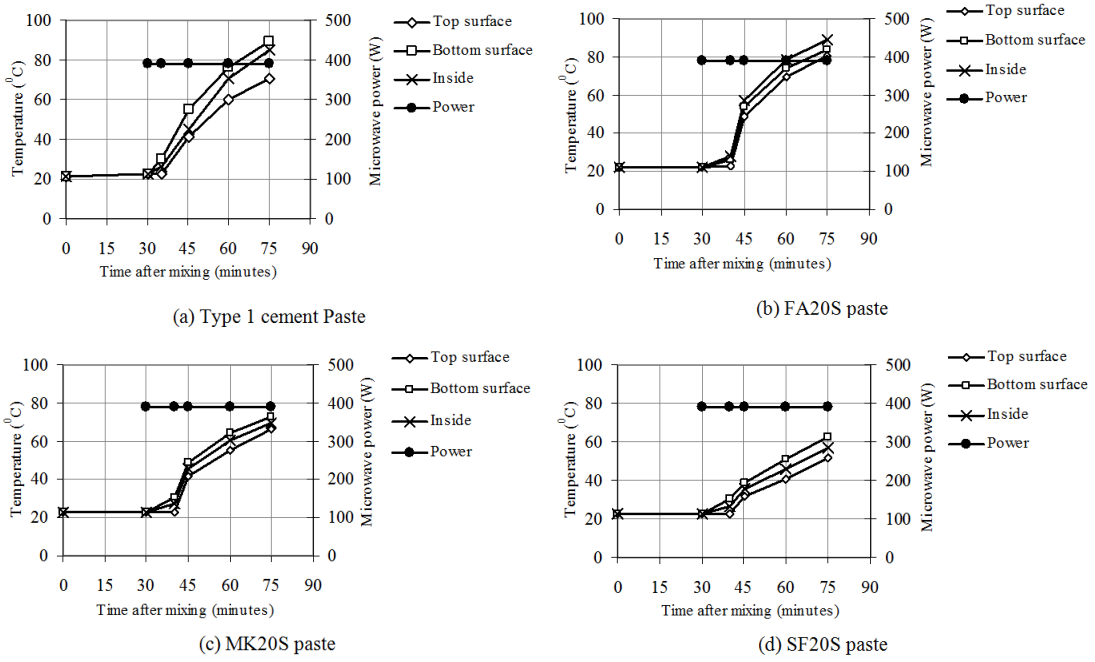

Figure 6. Temperature and power history during applying microwave energy of various cement pastes mixed with pozzolan materials.

that an increase in this reaction is accompanied by an increase in heat liberation or temperature rise. In Figure 6, we see that the bottom surface of the microwave-cured paste always has the highest temperature. The temperature of the top side is strongly affected by the rate at which water evaporates; but at the bottom surface, water evaporation takes place more slowly.

3.3 Morphology

The typical micrographs of FA20S, MK20S and SF20S pastes at the age of 4 hrs after mixing and being subjected to microwave energy at a microwave power of 390 W for 45 min are shown in Figure 7. The FA20S paste shows little difference among the microstructures at the three detecting times. Some ettringite rods and amorphous C_x-S_y-H_z fibers appear at 4 hrs, but none appear in the FA20S paste that was heated by microwave energy. This fact implies that microwave by can accelerate the pozzolan reaction and generate lath-shaped ettringite more often, which takes the place of rod-shaped ettringite. The MK20S formulation shows little difference between the water-cured and microwave-cured pastes. On the other hand, for the SF20S paste, microwave curing accelerates the reaction compared to the 4 h water curing.

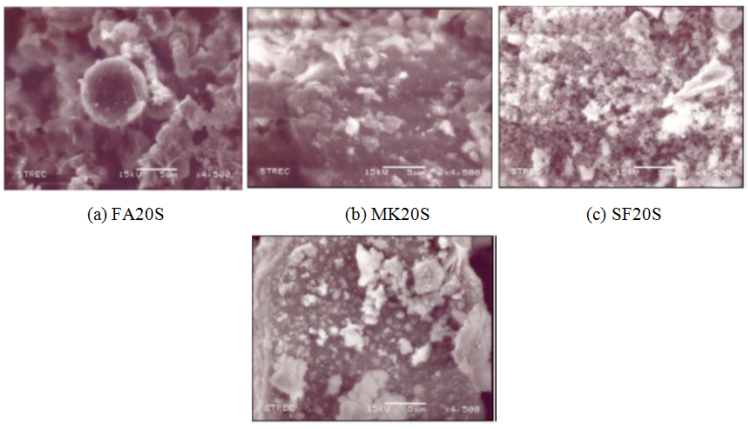

Figure 7. Micrographs of FA20S, MK20S and SF20S paste specimens at 4 hrs after microwave treatment compared to Type 1 cement paste specimen.

Finally, the paste at 28 days looks like a plate of C-S-H in which SF particles cannot be distinguished.

3.4 Atomic ratios of the pastes

Figure 8 shows the atomic ratio of Si/Ca versus Al/Ca for the pastes after microwave power of 390 W was applied for 45 min. In the case of the Type 1 cement paste, we have a tight cluster of points representing the Si/Ca and Al/Ca ratios (the Si/Ca ratios are in the range 0.220–0.263, while the Al/Ca ratios are in the range 0.079-0.091). These ratios determine the ratio of hydration products - calcium silicate hydrates (C_x-S_y-H_z) versus calcium silicate aluminates (C_x-A_y-H_z). The paste mixed with FA (FA20S) has a wider dispersion of Si/Ca versus Al/Ca than the Type 1 cement paste. The Al/Ca ratios of the FA20S increase due to the fact that the chemical composition of FA is mainly SiO_2 (47.80%) and Al_2O_3 (22.70%). The paste therefore generates more calcium silicate aluminates (C_x-A_y-H_z), which is reflected in its higher Al/Ca ratio compared to the Type 1 cement paste. However, the SiO_2 composition of the FA paste does not affect the calcium silicate hydrates (C_x-S_y-H_z) – Si/Ca ratio, which is similar to that of the Type 1 cement paste.

Similarly, the paste mixed with MK (MK20S) achieves a higher Al/Ca ratio than the Type 1 cement paste, because MK has a higher Al_2O_3 content. In contrast, the SF paste (SF20S) achieves a higher Si/Ca ratio than the Type 1 cement paste because SF is a silica-rich material. The Si/Ca ratios in the SF-paste shifted from 0.582 to 1.184.

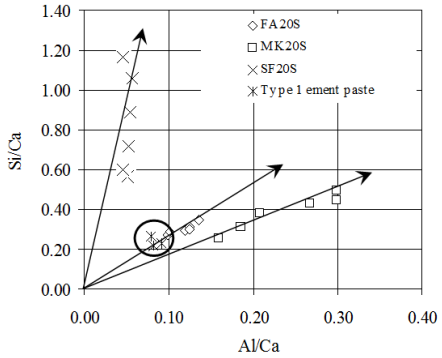

Figure 8. Ratios of Si/Ca and Al/Ca in FA20S, MK20S, SF20S, and Type 1 cement pastes following microwave heating.

3.4 Phase identification

X-ray diffractometry was used to determine the produced phases the hydrated cement products and the existence of crystalline coexisting phases. Figure 9 shows X-ray diffraction of FA20S, MK20S and SF20S after microwave curing at a power of 390 W had been applied for 45 min. The phases identified include calcium silicate hydrate (Ca_3SiO_5), calcium hydroxide ($Ca(OH)_2$), residual lime (CaO), and Xenotile ($Ca_6(SiO_3)_6(H_2O)$). As shown in Figure 9, microwave curing does not affect the phase characteristics of FA20S, MK20S, or SF20S in comparison with the Type 1 cement paste.

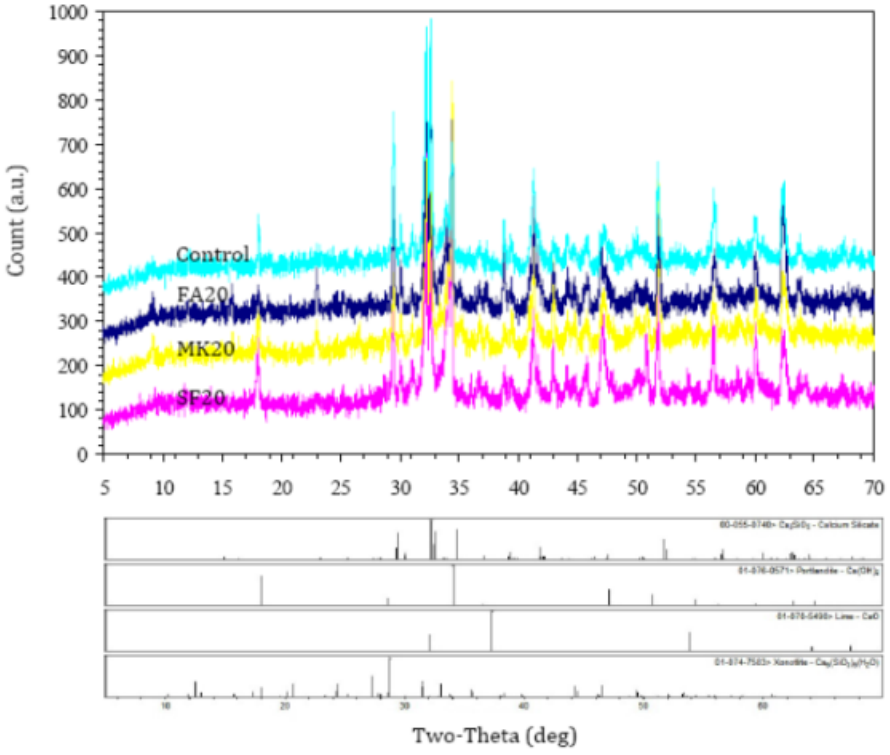

Figure 9. X-ray diffraction spectra of FA20, MK20, and SF20 specimens.

3.5 Mechanical properties of pastes

Curing at elevated temperatures encouraged rapid strength development within the pastes (Figure 10). The FA20S paste achieved a compressive strength of 4.1 MPa at 8 hrs, 9.2 MPa at 24 hrs, 25.1 MPa at 7 days, and 40.6 MPa at 28 days. The MK20S and SF20S pastes achieved 8-hr compressive strengths of 8.6 and 12.1 MPa, which exceeded the strength of the conventionally-cured pastes. The strength development of pastes containing pozzolan material was different from the control paste, with continuous development beyond 24 hrs. This effect is due to increased pozzolan (which produces secondary C-S-H content) and hydration reactions. Both of these reactions contribute additional heat which facilitates the later-age strength development of the pozzolan-containing cement pastes.

The compressive strength development of the pozzolan-containing pastes is related to their $Ca(OH)_2$ content, which may be determined from the weight loss of the samples when heated to 400-550°C as shown in Figure 11. The $Ca(OH)_2$ contents of the FA20S, MK20S, and SF20S cement pastes were 3.08, 2.36, and 1.59 wt%, suggesting that the SF-containing cement paste consumed more $Ca(OH)_2$ in pozzolan reactions, producing more C_x-S_y-H_z and resulting in greater compressive strength.

4. Relation between Microwave Energy and Compressive Strength of Pastes with or without Pozzolan Materials

Referring to the famous relationship described by Popovics (1990), the strength of concrete is inversely related to its water-to-cement mass ratio as shown in Equation 4.

$$f_c = \frac{K_1}{K_2^{w/c}} \tag{4}$$

In this equation, f_c is the compressive strength, *w/c* is the water-to-cement mass ratio, and K_1 and K_2 are empirical constants. The Richards model (Equation 5) is suitable for comparing the compressive strengths of pastes subjected to microwave and conventional (lime-saturated deionized water) curing techniques, because its behavior is similar to the strength development patterns observed when varying the curing technique.

$$Compressive\,strength^{Normal\text{-}cured} = \frac{a}{\left(1+\exp^{(b-c(Compressive\,strength^{microwave\ cured}))}\right)^{\frac{1}{d}}} \tag{5}$$

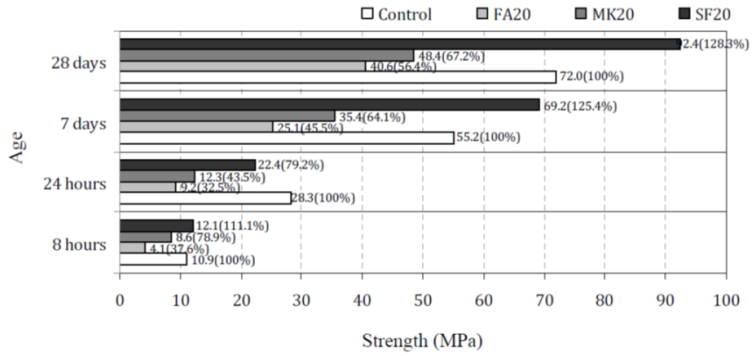

Figure 10. Compressive strength developments of control, FA20S, MK20S, and SF20S pastes following microwave heating.

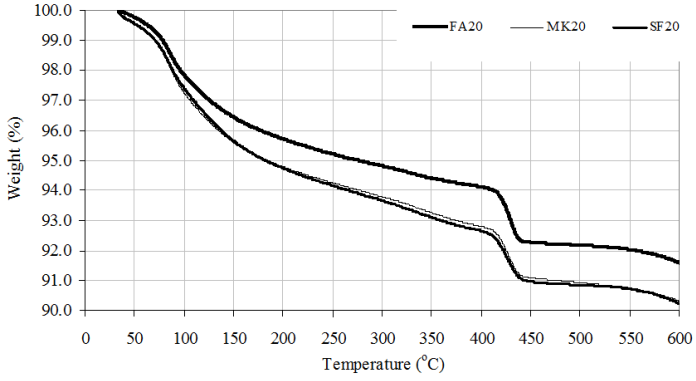

Figure 11. Thermal analysis results of pozzolan-containing pastes following microwave heating.

Here, $Compressive\ strength^{Normal\text{-}cured}$ represents the compressive strength of the conventionally-cured cement paste. The samples were tested at 8 hrs, 24 hrs, 7 days, and 24 days. $Compressive\ strength^{Microwave\text{-}cured}$ represents the compressive strength of samples undergoing microwave curing. The parameters *a, b, c,* and *d* are coefficients from the regression analysis.

Figure 12 displays the Richards model curve for the four compressive strengths of the control cement paste. The coefficients are summarized in Table 3. With respect to the water-to-powder mass ratios, the coefficient *a* appears to decrease in value when the applied energy, microwave power (W)×time of application (min), increases. This is because the temperature rise increases the degree of irregularity in the C–S–H structure and the presence of additional imperfections reduces its strength.

The regression coefficients *a, b, c,* and *d* are plotted with respect to temperature and energy input in Figure 12. The *a* coefficient was higher at lower energies, reaching a maximum at an energy level between 2.0 and 3.0 kJ. The *b* coefficient varied inversely with *a*, while *c* and *d* exhibited periodic variations.

5. Conclusions

In the study under microwave heating of pozzolan-Portland cement pastes at a very early age with a 2.45 GHz-multimode cavity at a power of 390 W for 45 min and cylindrical samples in ϕ 69.0 mm diameter × 4.0 mm high, we found that:

- The temperature increases monotonically during the microwave-curing process and reached a maximum temperature of 89°C FA20S paste, 72.9°C of MK20S paste, and 62.4 ° C of SF20S paste.
- FA20S and MK20S pastes exhibit little difference among the microstructures. On the other hand, for the SF20S paste the SF particles under microwave curing have dispersed more than with the 4-hr cement paste, while the paste at 28 days looks like a plate of C-S-H.
- Phases identified of FA20S, MK20S and SF20S pastes included calcium silicate hydrate (Ca_3SiO_5), calcium hydroxide ($Ca(OH)_2$), residual lime (CaO), and Xenotile ($Ca_6(SiO_3)_6(H_2O)$).
- Pastes containing pulverized fuel ash, metakaolin and silica fume materials was gained compressive strength development after 24 hrs and later ages and corresponded to a decreasing $Ca(OH)_2$ content.
- After analysis based on Abram's law, for the specimen size of cylindrical samples 41.0 mm in diameter and 34.0 mm tall, the highest compressive strength of cement-pozzolan pastes was obtained using a microwave energy level between 2.0 and 3.0 kJ.

Acknowledgment

The authors gratefully acknowledge the Thailand Research Fund (TRF contract No. MRG5580041) for supporting this research.

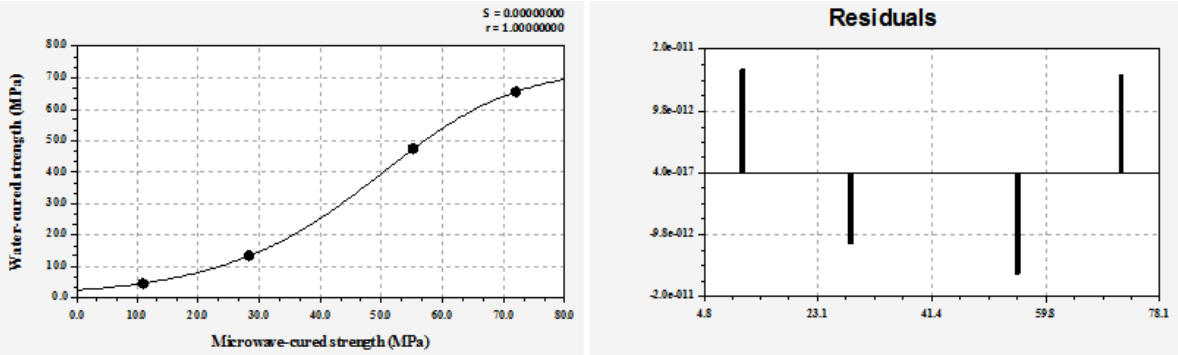

Figure 12. Regression and residuals for compressive strength of the Type 1 cement paste.

Table 3. Correlation coefficients for compressive strength of cement pastes.

Type of Paste	a	b	c	d
Control	73.431	5.270	0.096	1.540
FA20	74.364	-0.879	0.051	0.136
MK20	58.458	-1.227	0.059	0.125
SF20	129.579	-1.153	0.026	0.110

References

American Concrete Institute Committee. 2005. Building code requirements for structural concrete and commentary, American Concrete Institute, Farmington Hills, Michigan, U.S.A.

American Society for Testing and Materials. 2009a. Annual Book of ASTM Standard: Concrete and Aggregates, 4(2), Philadelphia, Pennsylvania, U.S.A.

American Society for Testing and Materials. 2009b. Annual Book of ASTM Standard: Cement; Lime; Gypsum, 4(1), Philadelphia, Pennsylvania, U.S.A.

Arunachalam, K. 2008. Characterization of a digital microwave radiometry system for noninvasive thermometry using a temperature–controlled homogeneous test Load. Physics in Medicine and Biology. 53 (14), 3883-3901.

Badogiannis, E., Kakali G., Dimopoulou, G., Chaniotakis, E. and Tsivilis, S. 2005. Metakaolin as a main cement constituent: Exploitation of poor Greek kaolins. Cement and Concrete Composites. 27 (2), 197-203.

Basak, T. and Durairaj, S. 2001. Numerical simulation on efficient microwave processing of thermoplastics with ceramic composites. Numerical Heat Transfer; Part A: Application. 57, 554-579.

Beall, F.C. 2007. Industrial applications and opportunities for nondestructive evaluation of structural wood members. Maderas: Cienciay Tecnologia. 9, 127-134.

Bhanja S. and Sengupta, B. 2003. Modified water–cement ratio law for silica fume concretes. Cement and Concrete Research. 33 (3), 447-450.

Chen, H., 2008. Simulation model for moving food packages in microwave heating processes using conformal FDTD method. Journal of Food Engineering. 88, 294-305.

Dongxu, L. and Xuequan, W. 1994. A study on the application of vacuum microwave composite dewatering technique in concrete engineering. Cement and Concrete Research. 24(1), 159-164.

Göksoy, E.O., James, C. and Corry, J.E.L. 2000. The effect of short-time microwave exposures on inoculated pathogens on chicken and the shelf-life of uninoculated chicken meat. Journal of Food Engineering. 45(3), 153-160.

Hewlett Packard Corporation. 1992. Dielectric Probe Kit 85070A. Palo Alto, CA: Research and Development Unit, Test and Measurements Laboratories.

Hutchison. R.G., Chang, J.T., Jennings, H.M. and Brodwin, M.E. 1991. Thermal acceleration of Portland cement mortars with microwave Energy. Cement and Concrete Research. 21, 795-799.

Jae-Hwan, P., Byung-Kook K., Jae-Gwan, P. and Yoonho, K. 2001. Effect of microstructure on the microwave properties in dielectric ceramics. Journal of the European Ceramic Society. 21(15), 2669-2672.

Kim, H.K. and Lee, H.K. 2011. Use of power plant bottom ash as fine and coarse aggregates in high-strength concrete. Construction and Building Materials. 25(2), 1115-1122.

Leung, K.Y.C. and Pheeraphan, T. 1995. Microwave curing of Portland cement concrete: Experimental Results and Feasibility for Practical Applications. Construction and Building Materials. 9, 67-73.

Li, W., Ebadian, M.A., White, T.L., Grubb, R.G. and Foster, D. 1994. Heat and mass transfer in a contaminated porous concrete slab with variable dielectric properties. International Journal of Heat and Mass Transfer. 37 (6), 1013-1027.

Metaxas, A.C. 1991. Microwave heating, Journal of Microwave Power and Electromagnetic Energy, 237-247.

Moukwa, M., Brodwin, M., Christo, S., Chang, J. and Shah, S. P. 1991. The influence of the hydration process upon microwave properties of cements. Cement and Concrete Research. 21, 863-872.

Makul N., Chatveera B. and Rattanadecho P. 2009. Use of microwave energy for accelerated curing of concrete: a review. Songklanakarin Journal Science and Technology. 31 (1), 1-13.

Orsat, V. 2007. Microwave-assisted drying of biomaterials. Food and Bioproducts Processing. 85(3C), 255-263.

Padma K.H., Suresh, M.K. and Thomas, J.K. 2009. Effect of WO_3 and MoO_3 addition on $LnTiTaO_6$ (Ln = Ce, Pr and Nd) microwave ceramics. Journal of Alloys and Compounds. 478 (1-2), 648-652.

Peyre, F., Datta, A. and Seyler, C. 1997. Influence of the dielectric property on microwave oven heating patterns: application to food materials. Journal of Microwave Power and Electromagnetic Energy. 32, 3-15.

Popovics, S., 1990. Analysis of concrete strength versus water-cement ratio relationship. ACI Material Journal. 87, 517-529.

Sgriccia, N. and Hawley, M.C. 1991. Thermal, morphological, and electrical characterization of microwave processed natural fiber composites. Composites Science and Technology. 67 (9), 1986-1991.

Taher, B.J. and Farid, M.M. 2001. Cyclic microwave thawing of frozen meat: experimental and theoretical investigation. Chemical Engineering and Processing. 40 (4), 379-389.

Venkatesh, M.S. and Raghevan, G.S.V. 2005. An overview of dielectric properties measuring techniques. Canadian Biosystems Engineering. 47, 15-29.

Verbeck, G.J. and Helmuth, R.A. 1969. Structures and physical properties of cement paste. Proceedings of the Fifth International Symposium on the Chemistry of Cement, Tokyo, Japan, October 7-11, 1968, 1-44.

Wittmann F.H. and Schlude F. 1975. Microwave absorption of hardened cement paste. Cement and Concrete Research. 5, 63-71.

Zhu, J., Kuznetsov, A.V. and Sandeep, K.P. 2007. Numerical modeling of a moving particle in a continuous flow subjected to microwave heating. Numerical Heat Transfer; Part A: Application. 52 (5), 417-439.